

**Investigation of an Alternative Crash Concept
for Composite Transport Aircraft using Tension Absorption**



P. Schatrow*) • M. Waimer*)

*) German Aerospace Center (DLR), Institute of Structures and Design, 70569 Stuttgart, Germany

Abstract

Transport aircraft made of CFRP have to provide an equivalent crashworthiness compared to today's aluminium aircraft designs. However, CFRP structures typically show brittle failure behaviour and limited energy absorption, whereas aluminium structures offer sufficient crashworthiness purely due to the ductile behaviour of metal. Specific crash designs have to be developed for CFRP fuselage structures that involve local crash devices for energy absorption and controlled failure mechanisms. Trigger mechanisms, energy absorbing devices and their positioning in the fuselage have to be defined.

In the past, several research activities concentrated on the 'bend-frame' concept that specifies a cargo crossbeam of high strength to allow energy absorption by progressive crushing below this crossbeam in the sub-cargo area. The research work on the bend-frame concept identified critical drawbacks which are mainly found in the mass penalty due to the need of a massive cargo crossbeam and frame design that is able to sustain the crush forces in the sub-cargo area.

In this context an alternative crash concept was investigated that concentrated on tension absorption mechanisms. The focus of this study was on a crash design that provides smooth energy absorption and a lightweight structural design leading to a significantly reduced mass penalty due to the crash sizing.

Numerical simulations were performed on the basis of a generic CFRP fuselage section. The tension absorbers are located in the cargo and the passenger crossbeams that benefit from the tension loads acting in the crossbeams. This is due to the global bending of the sub-cargo structure (cargo crossbeam) and the ovalisation of the fuselage respectively frame structure (passenger crossbeam). Further energy is absorbed in the frame structure.

In the scope of this numerical study potential tension absorber characteristics were determined that led to an optimised and smooth crash kinematics of the fuselage section. The statically pre-sized fuselage structure was adapted to the crash loads to identify the mass penalty caused by the crash sizing. Furthermore, the passenger loads were analysed and assessed with respect to potential injury risks. The results of this simulation study indicate significant benefits for the tension absorption concept compared to the bend-frame concept. The simulations were performed using the commercially available explicit FE code Abaqus/Explicit and the kinematics model approach.

Keywords:

CFRP transport aircraft • crashworthiness • tension absorption • finite element simulation • crash kinematics assessment • cargo loading

1 Introduction

Crash behaviour of nowadays metallic aircraft

Several drop tests of aircraft fuselage sections, cut from metallic transport aircraft, were performed in the past to investigate the energy absorption behaviour in

emergency landing conditions of transport aircraft [1], [2], [12], [20], [22], [23], [24], [25], [32], [38], [39]. The drop tests were conducted with different impact velocities and with different loading conditions. The cross section of the fuselage structures can be divided in a passenger zone and in an energy absorbing zone. The passenger zone, located above the cabin floor, is

supposed to be undamaged while the energy absorbing zone, located below the cabin floor, is supposed to absorb the kinetic crash energy of the fuselage section. In the mentioned drop tests, several energy absorbing failure mechanisms which absorbed most of the kinetic energy of the fuselage section can be identified in this absorbing zone below the cabin floor.

The first energy absorbing area, according to the crash sequence, is located below the cargo floor. The kinetic energy of the metallic fuselage sections is absorbed in this area by plastic deformation of the frame, cargo crossbeam and skin as well as by damage and failure in the frame, the sub-cargo area and in the joints.

The second energy absorbing area is located in the frame above the cargo floor and below the lower connection of the vertical oriented support struts of the cabin floor. According to the drop test results, most of the kinetic energy is absorbed here by frame bending with large rotations on high moment level resulting in significant energy absorption capability. The metallic frames achieved high absorbing moment level solely by its ductility.

The third energy absorbing area is located directly below the cabin floor which includes the frame and the vertical oriented support struts. High energy absorption can be achieved by plastic deformation of the frame and of the vertical oriented struts in this area.

Despite of this beneficial crash behaviour obtained by the metallic ductility, the overall efficiency (especially with respect to other disciplines) of future aircraft can be further improved by replacing aluminium alloys in aircraft primary structures with composite materials and composite designs. With respect to the crash aspect, safety regulations require for transport aircraft made of carbon fibre reinforced plastics (CFRP) an equivalent crashworthiness compared to nowadays transport aircraft which are made of aluminium alloys [41]. The primary challenge of using CFRP for crashworthy aircraft structures is the brittle behaviour and the propensity towards uncontrolled failure with little energy absorption compared to aluminium structures. Sufficient energy absorption in CFRP aircraft can be achieved by the installation of crash devices, which are designed for specific loading conditions, in the fuselage structure where failure is expected due to bending, crushing or tension loads.

Bend-frame crash concept for composite aircraft

In several research studies a so called ‘bend-frame’ crash concept for composite transport aircraft was investigated [3], [6], [7], [29], [33], [37]. This concept is usually characterised by a cascading crash scenario in which the individual crash devices are activated successively during the crash sequence. The energy absorption starts at the impact point of the lower fuselage shell by progressive crushing of vertical orientated structural elements which are installed below the cargo floor. The cargo crossbeam provides high stiffness respectively strength and has to sustain high bending loads (‘bend-frame’) in this crash phase due to the crush loads of the sub-cargo structure. A significant amount of the kinetic crash energy is absorbed in this cargo structure in the first phase of the crash sequence. In the next step increasing crash loads activate the crash devices of the second area located in the frame below the lower connection of the vertical support struts. Here, energy can be absorbed by bending failure of the frame structure. Finally, in the third step the crash loads activate the crushing of the vertical oriented support struts below the cabin floor.

This crash cascade that includes the bend-frame concept requires systematic definition of the trigger loads in the crash devices of each area to ensure a controlled crash scenario (stepwise triggering). Research work [33] identified critical mass penalty of the bend-frame concept due to the need of a massive cargo crossbeam and frame design to achieve progressive crushing of the structural elements below the cargo floor. As a result the mass of the crashworthy frame and cargo crossbeam design is significantly higher compared to its static design.

Alternative crash concept for composite aircraft

Further research on aircraft crashworthiness indicated high tension forces in two areas of the fuselage section which can be used for energy absorption [27], [33]. In the first area located in the connection between the frame and the cabin floor high tension forces occur due to the ‘ovalisation effect’. The ovalisation of the fuselage section occurs due to the tendency of the fuselage structure to deform to an oval shape caused by the crash loads [33]. In the second area, located in the cargo floor (cargo crossbeam), high tension forces occur due to the bending loads in the sub-cargo structure [27].

According to this effect an alternative crash concept for composite transport aircraft was developed whose

main absorption mechanism is based on tension absorption. The focus of this study was to achieve maximum energy absorption by tensile failure and to avoid energy absorption concepts which are combined with additional mass penalty (e.g. crushing of vertical oriented structural elements in the sub-cargo area which requires massive backing structure). Besides this, more realistic (reduced) energy absorption requirements should be made for CFRP structures with unfavourable failure modes (e.g. bending absorption in the CFRP frame) to develop a crash kinematics with lightweight design, hence to keep the lightweight benefits of a CFRP fuselage compared to an aluminium fuselage.

Kinematics modelling approach

Different FE modelling approaches can be used to develop and assess new crash concepts on preliminary design level. The kinematics model approach was applied in this study, which is described and discussed in the context of other modelling approaches in [33], [34], [35]. The feature of this kinematics modelling is to combine the benefits of hybrid simulation techniques (e.g. DRI-KRASH [28]) and of detailed FEM techniques. Regions in the fuselage section where damage and failure is expected are represented by macro elements. Other regions which are expected to remain undamaged are discretised with coarse mesh density and linear-elastic material formulations. On the one hand, time expensive calculation processes, such as simulation of crushing or frame bending failure, are represented by macro elements whose failure characteristics can be described by force-displacement or moment-rotation curves. On the other hand, in the region of coarse discretisation and linear-elastic material formulations the kinematics model approach still provides sufficient accuracy to represent detailed structural effects such as frame-skin interaction or instabilities. The input-characteristics of the macro elements can be obtained from experimental test results, from detailed FEM simulations or from reasonable assumptions. The kinematics modelling approach allows fast and efficient assessment of required absorber characteristics, of structural and passenger loads, and of the overall fuselage section crash behaviour with different loading conditions.

Figure 1 illustrates the main approach of the kinematics modelling in the context of the developed tension crash concept. On the left side of Figure 1 a

generic full CFRP transport aircraft fuselage section is shown, and on the right side its representation in the kinematics modelling approach. Specific crash devices are installed in the fuselage structure to compensate the brittle failure behaviour of CFRP at complex loading conditions. According to the alternative tension crash concept these crash devices have to be designed mainly for tension absorption as well as for bending absorption. The location of the crash devices and its potential physical design are illustrated on the left side of Figure 1. In the kinematics modelling approach the crash devices are represented by idealised force-displacement and moment-rotation input-characteristics with loading curve and with unloading/ reloading behaviour. On the right side of Figure 1 exemplary input-characteristics and macro architectures are illustrated which represent the failure behaviour of the crash devices.

In the cargo floor high tension forces occur due to the bending loads acting on the sub-cargo structure. One potential physical design of the tension absorbers in this area is represented by a metallic device which absorbs kinetic energy by plastic decreasing of the tube diameter (Figure 1c) [9]. In [8] an overview of further tension absorption concepts based on elongation of metallic structures is given. In the kinematics modelling approach this crash device is represented by two serial connector elements to allow the modelling of articulated connection on both ends of the tension absorber. The connector behaviour is represented by a force-displacement characteristic that includes loading and unloading/ reloading curves.

In the cabin floor high tension forces occur due to the deformation of the fuselage section to an oval shape (ovalisation effect). In the first crash phase, and during the unrolling of the lower frame, high tension forces occur in this connection. One potential crash device for this connection is represented by bearing failure in which bolts or joints are pulled through a laminate (Figure 1a). In [26], [30], [31] tension absorption concepts are described which are based on bearing failure of composite materials. In the kinematics modelling approach this crash device is represented by a connector element with force-displacement and moment-rotation characteristics.

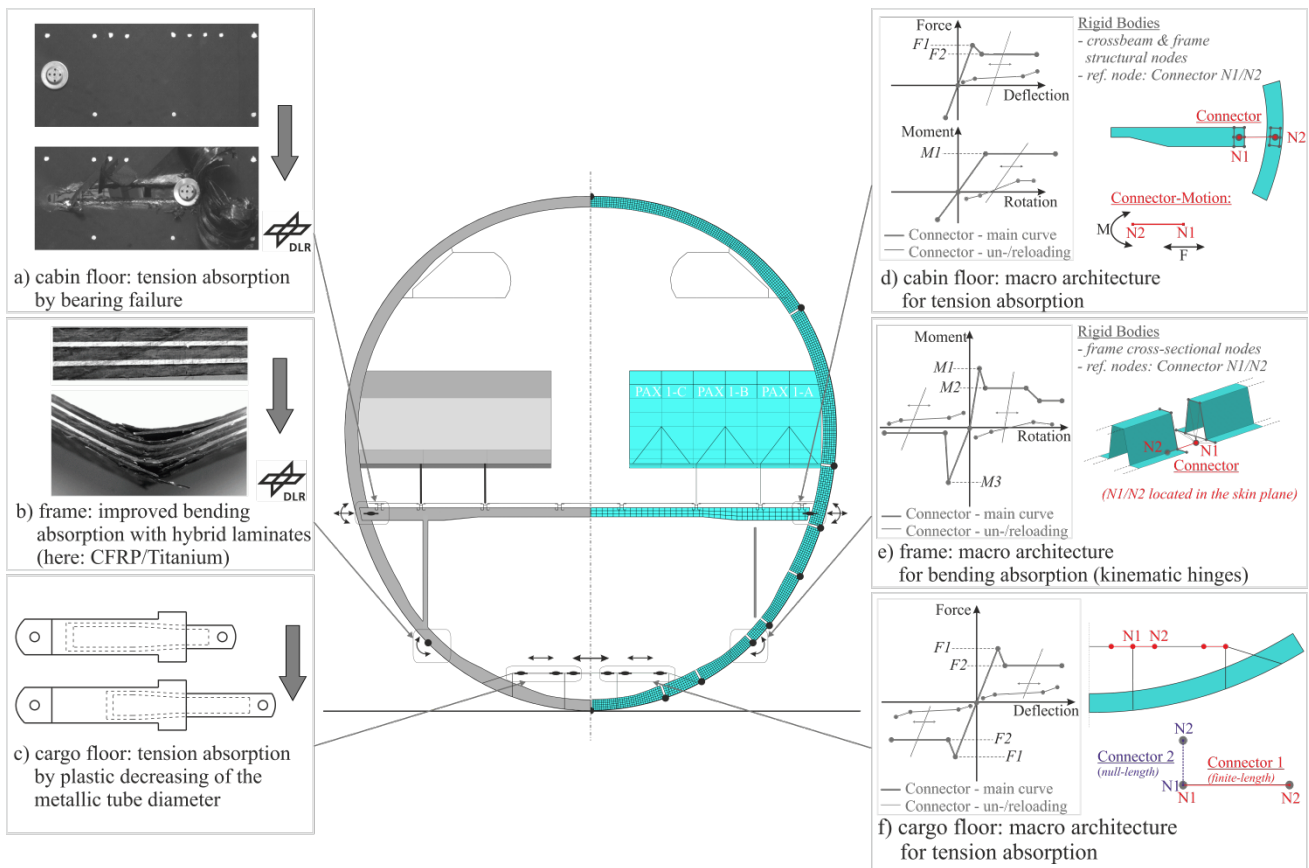


Figure 1: Tension crash concept. Left: potential absorption mechanisms. Right: macro architectures (kinematics modelling)

Several research work show that bending absorption in CFRP frame structures is generally limited due to the unfavourable material failure behaviour in this loading condition [4], [5], [34], [40]. Therefore moderate requirements should be defined for bending absorption in CFRP frames. One potential physical crash device for crashworthy frames with increased bending absorption is represented by hybrid CFRP/titanium laminates (Figure 1b) [34]. In the kinematics model the frame failure is represented by so called 'kinematic hinges'. The macro architecture for kinematic hinges is described by a cut in the frame whose cross sections are reinforced by rigid bodies. Each of the kinematic hinges represents potential frame failure locations. The approximate locations of the kinematic hinges in the frame are known from several drop tests which were previously described. A more accurate definition of the kinematic hinge locations is determined by evaluating the strain distribution along the frame and placing the kinematic hinges at positions of local strain extremum [35]. The connector element behaviour of the kinematic hinges is described by a moment-rotation characteristic that includes loading and unloading/ reloading curves.

2 Development of the tension crash concept

Several drop tests of fuselage sections were performed in the past to investigate the energy absorption behaviour of typical passenger transport aircraft [12], [22], [23], [24], [38], [39]. In general, the obtained crash kinematics of the considered typical fuselage sections can be classified in two categories, as exemplarily depicted in Figure 2. In the first crash kinematics frame failure occurs at the impact point and almost symmetrically between 40°-60° in circumferential direction starting from the impact point on both sides resulting in an unrolling kinematics of the lower fuselage section (Figure 2a). In the second crash kinematics multiple frame failure occurs in the lower fuselage section and further frame failure occurs below the vertical support struts which results in a flattening kinematics of the lower fuselage shell (Figure 2b). Both crash kinematics show the natural behaviour of typical fuselage structures which are impacted on a rigid surface. These natural crash kinematics should be regarded in the development of new crash concepts to achieve a lightweight crashworthy structural design.

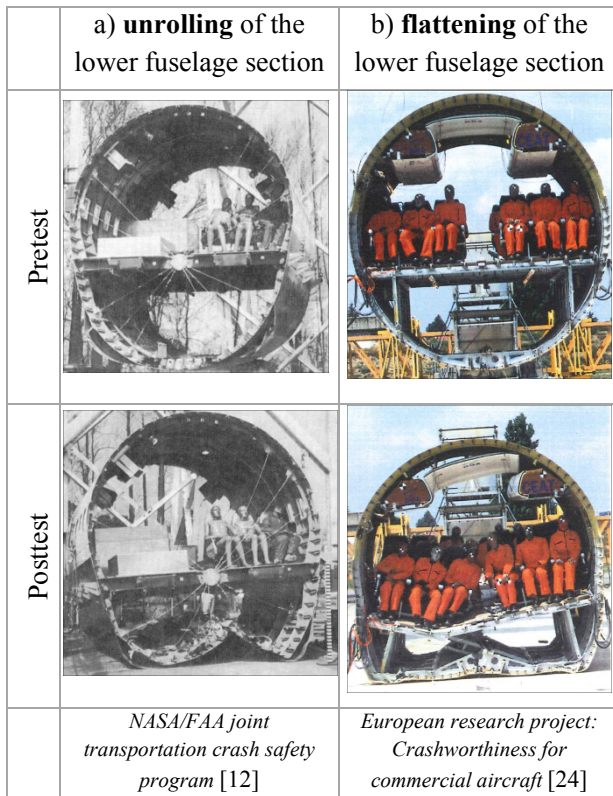


Figure 2: Crash kinematics with flattening and unrolling of the lower fuselage section

Both general crash kinematics are considered in the presented research work on the alternative crash concept based on tension absorption. However, further discussion in this paper is focused on the flattening kinematics depicted in Figure 2b. Results of the unrolling kinematics will be published soon in a journal research article.

The crash kinematics of the tension crash concept was developed on the basis of a statically pre-sized generic single aisle full CFRP transport aircraft design, which was provided by Airbus in the scope of this research cooperation. A 2-bay fuselage section is considered under purely vertical impact conditions.

The length of the fuselage section is 1270 mm with a frame pitch of 635 mm. The frames are equipped with an asymmetric omega-shaped cross section as depicted in Figure 1e. The fuselage cross section is described by four different radii between 1887 mm and 2609 mm. The vertical position of the cargo floor is about 300 mm (distance between the lower skin and the cargo floor level). All structural parts are modelled with shell elements, except the stringers, sub-cargo and seat struts which are modelled with beam elements.

The total mass of the 2-bay fuselage section is 1430.4 kg. The fuselage section model is equipped with two

seat rows of triple seats. Standard passenger masses of 77 kg were scaled to 68.5 kg to reasonably match the seat pitch with the frame pitch in the simulation model. In Table 1 the mass balance of the simulation model is shown. An initial velocity of 6.7 m/s (22 ft/s) in vertical direction was assigned to all nodes of the fuselage section model.

Table 1: Mass balance of the simulation model

| Structural element | Mass |
|-------------------------------------------------|-------------------------|
| 89% Passengers (different frame and seat pitch) | 12 * 68.5 kg = 822.4 kg |
| Hatracks | 2 * 75.8 kg = 151.6 kg |
| Seats | 131.7 kg |
| Systems | 72.3 kg |
| Structure | 252.4 kg |
| <hr/> | |
| 2-bay simulation model | 1430.4 kg |

Discrete rivets or other joints are not modelled in detail in this simulation model. Instead the structural parts were joined using tie constraints. A general contact between the fuselage skin and the impact surface is defined with a friction coefficient of 0.4.

The 2-bay fuselage FE-model contains approximately 40,300 nodes and 40,000 elements with 32,500 shell elements, 5800 strain bar elements, 1700 beam elements, macro elements and mass elements. The total number of variables is approximately 220,000. The explicit simulations were performed with the commercially available FE-code Abaqus/Explicit V6.11-1 on one CPU of a Linux-Cluster. The simulation time is 200 ms, with an initial time increment of 1e-03 ms, and led to a calculation time of about 11 hours.

In Figure 3 the input-characteristics of the macro elements are illustrated. The maximum bending loads in the frame occur at the impact point in the kinematic hinges (A) and below the connection of the vertical support struts in the kinematic hinges (D). According to the crash kinematics in Figure 2b further frame failure can occur between the impact point (A) and the connection of the vertical support struts (D). These additional frame failure locations are represented in the simulation model by kinematic hinges (B) and (C). The accurate locations of the kinematic hinges can be determined by measuring and assessing of the strain along the frame. According to this procedure the kinematic hinges are located at positions of maximum strain.

In the kinematic hinges, the bending stiffness S_ϕ , the opening trigger moment M_1 and the closing trigger moment M_3 of the macro elements were adapted to the surrounding frame structure using detailed FE analysis as described in [33], [35]. The post-failure absorption level for opening moment loading (M_2) and for closing moment loading (M_4) are defined constantly at 30 % of the corresponding trigger moment and correspond to a low energy absorption capability of the frame.

In the cabin floor, the tensile stiffness S_{u*} of the tension absorber (d) is adapted to the tensile stiffness of the passenger crossbeam, while the trigger force F_{1*} corresponds approximately to the ultimate load of the static sizing. The constant absorption force level F_{2*} is defined at 70 % of the trigger force F_{1*} . The ratio of 70 % between the steady state absorption force and the trigger force is a typical value for bearing failure of composite laminates as it can be observed from experiments performed in [26], [30], [31]. The rotational stiffness of the cabin floor absorbers were modelled linear-elastically about the x-axis (flight direction).

In the cargo floor several tension absorbers (a), (b), (c) are placed in series. The tensile stiffness S_u of the tension absorbers (a), (b) and (c) was assumed to be the same as for the cabin floor absorber. A detailed sizing of the cargo crossbeam was not available in the preliminary design process so that detailed stiffness values could not be derived from the static sizing. The constant absorption force level F_2 was chosen in this way that the remaining kinetic energy, that is not absorbed in the cabin floor tension absorbers (d) and in the frame kinematic hinges (A), (B), (C) and (D), is absorbed in the cargo floor tension absorbers. According to this approach a significant amount of energy is absorbed by tension loads. Finally, the trigger force F_1 was determined with the relation $F_1 * 0.7 = F_2$. The tension absorbers in the cargo floor are equipped with a stop option to achieve the desired crash kinematics which is characterised by multiple frame failure as shown in Figure 2b. The stop option limits the maximum displacement in each of the tension absorbers and allows activation of several tension absorbers which are arranged in series. The stop option is defined by a force increase to a level at 125 % of the trigger force. The absorption displacement up to the stop force increase in each absorber of the cargo floor is limited to $u_{abs} = 55$ mm. The macro element rotation of the cargo floor

tension absorber is free about the x-axis (flight direction).

In this crash scenario, based on an initial impact velocity of 22 ft/s, the vertical support struts between the cabin floor and the frame do not participate to the energy absorption, therefore they are modelled with linear-elastic input-characteristics. The rotation of the vertical support struts is fixed about the x-axis (flight direction).

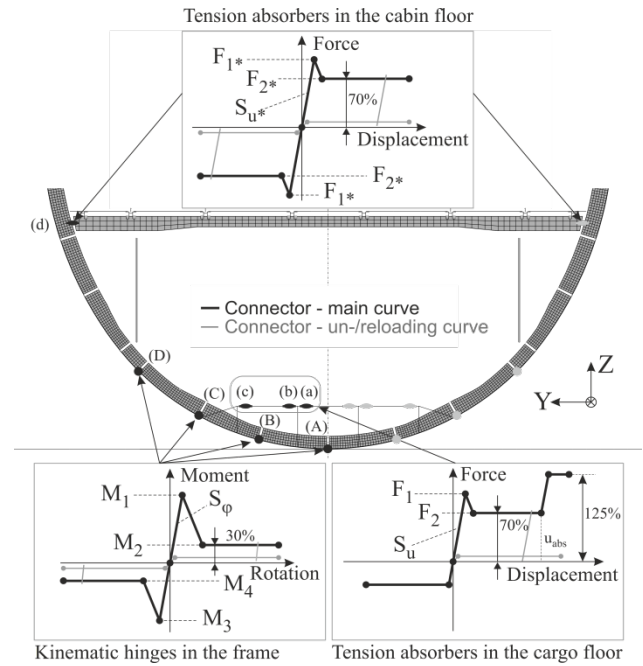


Figure 3: Input-characteristics for the macro elements representing structural failure

In Figure 4 the sequence of the crash kinematics with multiple frame failure and flattening of the lower fuselage section is shown. In the first crash phase (up to $t = 50$ ms), the kinematic hinges at the impact point (A) fail which causes the triggering of the tension absorbers (a) in the cargo floor. Subsequently, increasing crash loads and deformations lead to the triggering of the kinematic hinges (D) and the cabin floor tension absorbers (d) at approximately the same time. In the subsequent crash phase kinetic energy is absorbed in parallel by the frame bending mechanism of the kinematic hinges (A) and (D) as well as by the tension absorbers (a) in the cargo floor and (d) in the cabin floor. Approximately at $t = 54$ ms the inner tension absorber (a) in the cargo floor reaches its maximum displacement due to the stop option with correspondent force increase to 125% of the trigger force. This effect stops the bending rotation of kinematic hinge (A) and initiates the triggering of the tension absorber (b), and consequently frame bending

failure of the kinematic hinges in (B). Figure 4b shows the state ($t = 100$ ms) with activated tension absorbers (b) and kinematic hinges (B). At this state further energy is still absorbed by frame bending in the kinematic hinges (D). In the last crash phase, the kinetic energy is absorbed in the kinematic hinges (C) by further frame failure. This simulation result shows that the definition of the stop option in the tension absorbers (a), (b) and (c) allows to control the flattening kinematics in the lower fuselage shell with correspondent frame failures.

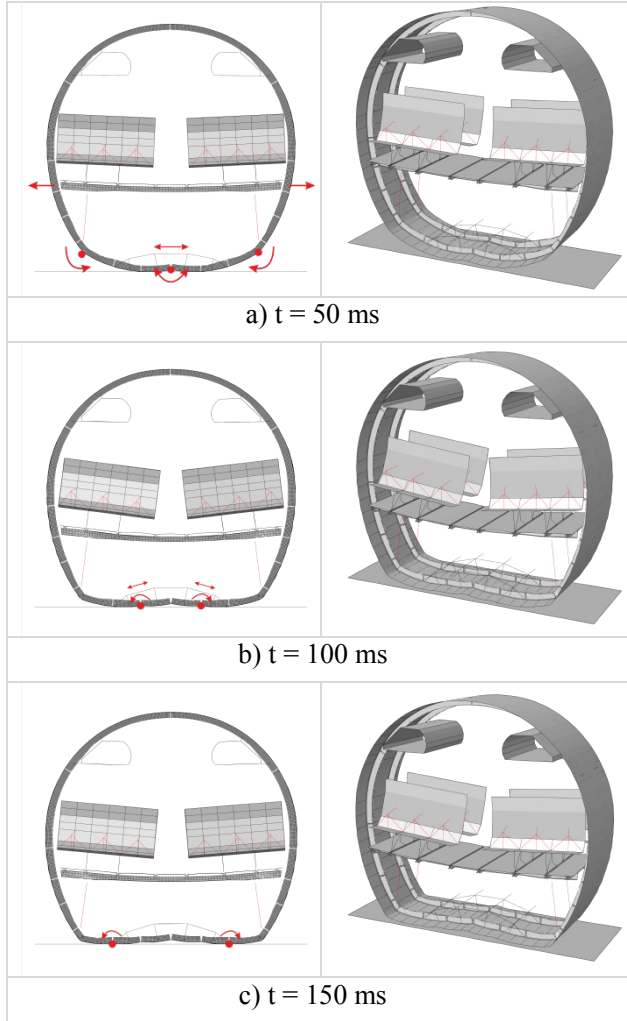


Figure 4: Flattening crash kinematics of the fuselage section

Energy balance

The energy balance is described using the general equations (1) and (2):

$$E_{TOT} \approx E_I + E_{KE} + E_{FD} - E_W, \quad (1)$$

$$E_I \approx E_E + E_{DMD}, \quad (2)$$

At $t_0 = 0$ ms the total energy is equal to the initial kinetic energy:

$$E_{TOT}^0 = E_{KE}^0 \quad (3)$$

At $t_1 = 200$ ms the energy balance is represented by:

$$E_{TOT}^1 \approx E_I^1 + E_{KE}^1 + E_{FD}^1 - E_W^1 \quad (4)$$

Since the total energy of the system is constant, combining the equations (3) and (4) results in:

$$E_{TOT}^0 = E_{TOT}^1$$

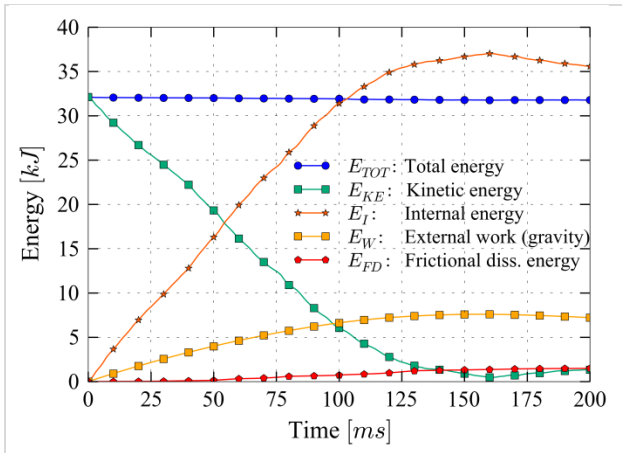
$$E_{KE}^0 \approx E_I^1 + E_{KE}^1 + E_{FD}^1 - E_W^1$$

$$E_{KE}^0 + E_W^1 \approx E_I^1 + E_{FD}^1 + E_{KE}^1 \quad (5)$$

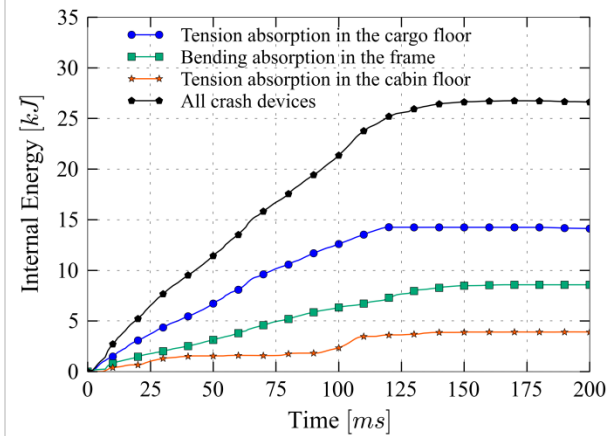
In Figure 5a the energy balance of the simulation model is shown. The total energy E_{TOT} is constant at 32.1 kJ. At the final crash state ($t_1 = 200$ ms), the initial kinetic energy and the external work $E_{KE}^0 + E_W^1$ (100 %) are transformed to the internal energy E_I^1 (90.5 %) and to the frictional dissipated energy E_{FD}^1 (3.8 %). A remaining kinetic energy E_{KE}^1 (3.4 %) is in the fuselage structure at this final state of the simulation. Furthermore, neglected energies (2.3 %) as described previously are in the system and represent the flaw size of equation (5).

Noticeable is the smooth decreasing of the kinetic energy during the whole crash sequence which is equivalent to minimum acceleration loadings of the passengers and minimum crash loads for the fuselage structure.

In Figure 5b the absorbed energies of the individual crash devices are shown. With respect to the initial kinetic energy and the external work ($E_{KE}^0 + E_W^1$) the amount of the absorbed energy in the cargo floor tension absorbers is 35.9 % (14.1 kJ), and of the cabin floor tension absorbers 9.9 % (3.9 kJ). The amount of the absorbed energy in the kinematic hinges (A) and (B) is 6.7 % (2.6 kJ) and in the kinematic hinges (C) and (D) 15.1 % (5.9 kJ). In total, about 67.6 % (26.5 kJ) of ($E_{KE}^0 + E_W^1$) were absorbed by the macro models of tension absorption and frame failure. The internal energy (67.6 %) of the macro elements consists of the elastic strain energy (6.2 %) and of the energy dissipated by damage (61.4 %). The amount of elastic strain energy in the linear-elastically modelled fuselage structure, except the macro elements, is 22.0 %. The elastic strain energy of the fuselage section model and the energy dissipated by damage are not shown in the diagram.



a) Energy balance



b) Internal energy in the crash devices

Figure 5: Energy output

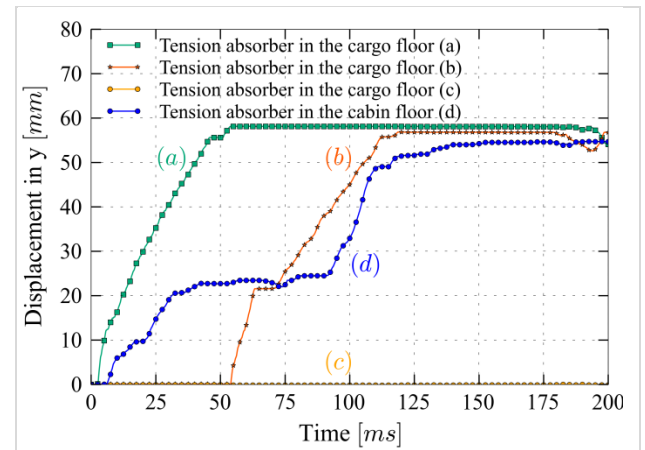
Output of the macro elements (displacement and rotation)

The output data of the macro elements in the crash devices can be used to derive characteristics and requirements for the physical crash devices. The simulation model provides almost symmetric crash kinematics therefore only output data of the macro elements located on one side of the simulation model are presented. Figure 6a shows displacement-time plots of the tension absorbers in the cabin floor (d) and in the cargo floor (a), (b), (c). The total displacement in each of the tension absorbers in the cargo floor (a) and (b) is approximately 57 mm ($u_{abs} = 55$ mm). The tension absorber (c) did not trigger in this crash scenario. The tension absorber (c) could be activated by reducing the maximum displacement u_{abs} in the tension absorbers (a) and (b). The plot shows the activation of the stop option in the tension absorber (a) approximately at $t = 54$ ms, which leads to the triggering of the tension absorber (b). In the further crash phase tension absorber (b) reaches the displacement u_{abs} of the stop force increase (approximately at $t = 110$ ms), but the

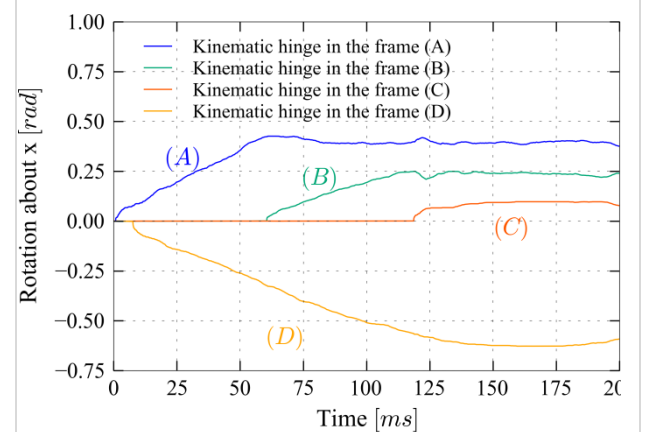
remaining kinetic energy is not sufficient to achieve subsequent triggering of tension absorber (c).

The maximum displacement in the tension absorber of the cabin floor (d) is 55 mm. It is activated for the first time at about $t = 5$ ms and for the second time at about $t = 105$ ms.

The bending rotations of the kinematic hinges (A), (B), (C) and (D) are given in the rotation-time plot shown in Figure 6b. According to the flattening kinematics the kinematic hinges (A), (B) and (C) trigger successively in positive direction. The kinematic hinge (D) triggers in negative direction according to the closing bending rotation. Table 2 shows the maximum bending rotations in the kinematic hinges (A), (B), (C) and (D).



a) Tension macro elements in the cargo floor (a), (b), (c) and in the cabin floor (d)



b) Kinematic hinges (A), (B), (C) and (D) in the frame

Figure 6: Displacement and rotation output data

Table 2: Maximum bending rotation in the kinematic hinges (A), (B), (C) and (D)

| Kinematic hinge | Bending rotation [rad] ([degree]) |
|-----------------|--------------------------------------|
| (A) | 0.43 (24.6) |
| (B) | 0.25 (14.3) |
| (C) | 0.1 (5.7) |
| (D) | -0.63 (-36.1) |

Assessment of the structural loads in the frame

In the scope of this simulation study the focus of the structural loads was on the frame which is the most important crash relevant structure. Loads along the frame structure were assessed by measuring the strains along the inner flange of the frame. The strain was measured by using bar elements of negligible stiffness which are positioned at the frame flanges.

The longitudinal strains were checked with respect to the given failure criteria and the statically pre-sized frame structure was re-sized according to the most critical strains in the inner frame flange. All results of the fuselage section simulation model given in this paper are with respect to the final crashworthy frame sizing.

Figure 7 depicts overall and state plots of all longitudinal strains which are determined by the bar elements along the frame. The crashworthy frame design provides a distribution of stiffness along the frame according to the crash loads in the individual regions. This frame profile distribution also distinguishes in different failure strains for tension and compression respectively opening and closing bending which is observable in Figure 7 in a bandwidth of different minimum and maximum failure strains. Curves of bar elements for strain measurement which are located directly in kinematic hinges indicate by abrupt increase the triggering of the

kinematic hinges. The kinematic hinges (A) triggers immediately after the first impact and the kinematic hinges (D) trigger at about 7.5 ms after the first impact. The kinematic hinges (B) trigger at approximately $t \approx 62$ ms and the kinematic hinges (C) at $t \approx 124$ ms in opening direction. Triggering of the kinematics hinges (B) and (C) occurred slightly asymmetric in the fuselage section which can be seen in Figure 7 in two different abrupt strain increases for the kinematics hinges. In the first crash phase the kinematic hinges (B) are loaded in closing direction up to the strain limit of the closing direction, before they finally trigger in an opening direction.

Few strain curves clearly exceed the failure strain values. These strains are influenced by rigid bodies in the kinematic hinges and at the passenger beam connection. Based on the selected modelling approach these artificially high strain values were not considered in the assessment of the structural loads.

In addition, Figure 7 shows state diagrams which plot the strain distribution along the frame of one state in a circle diagram against the circumferential angle of the fuselage section. Critical frame regions in which failure strain limits are exceeded can be visualised with these plots. The individual failure strain limits of all frame profiles along the frame are plotted in the diagrams. Strains which represent kinematic hinges are marked with a white circle. As can be seen from the state diagrams no significant exceeding of the strain limits occur due to the adaptation of the frame design, except some strains in the upper fuselage section at $t = 70$ ms and close to the passenger crossbeam connection at $t = 100$ ms. Despite these strain exceeding, further adaptation of the crashworthy frame design was not considered in this preliminary design study as further crash load cases have to be regarded first before a more detailed crash sizing is reasonable.

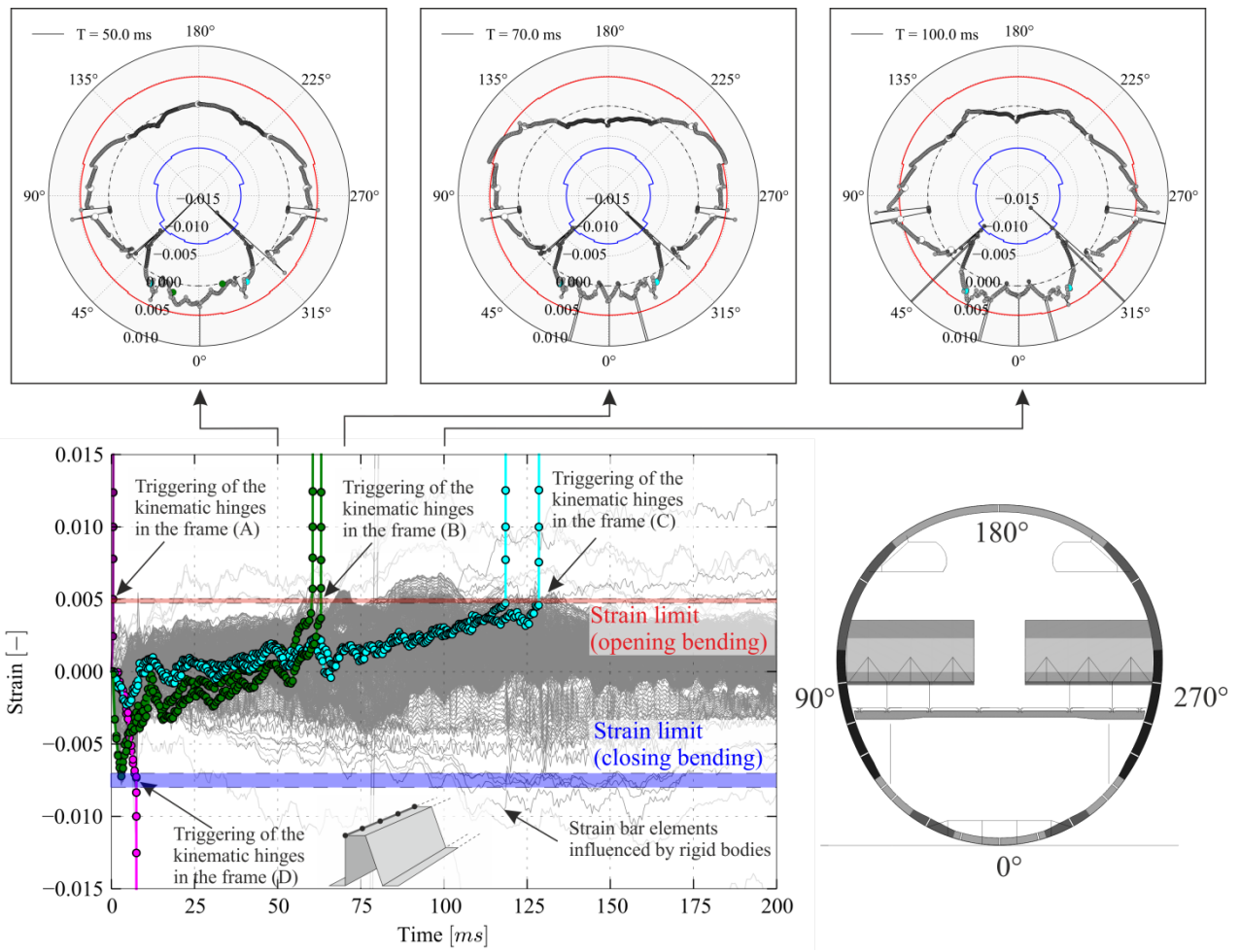


Figure 7: Circumferential strain in the inner flange of the frame (state plots and overall plot)

Assessment of structural loads in the cargo and cabin floor

The cargo floor framework structure essentially contributes to the tension crash concept as its structural integrity has to remain intact during the crash event to maintain the bending mechanism that leads to tension forces in the cargo crossbeam. The forces in the cargo crossbeam and especially in the vertical struts have to be checked and assessed to provide feasibility of the tension crash concept.

In Figure 8a the longitudinal forces in the vertical struts of the cargo floor framework are illustrated. The unfiltered output data were sampled with a frequency of 2 kHz and afterwards filtered with a Butterworth filter and a cut-off frequency of 0.1 kHz. The unfiltered maximum force in compression direction of the inner struts (1) is -11 kN and in tension direction $+4$ kN, while the maximum filtered force in compression direction is -9 kN. The maximum unfiltered force in compression direction of the outer struts (2) is -18.5 kN, while the maximum filtered value is -13 kN. The force in the outer vertical struts (2) is higher compared to the inner vertical struts (1).

The (horizontal) tension absorber forces in the cargo and the cabin floor are shown in Figure 8b. The cargo floor tension absorbers (a) and (b) trigger in series at a load level of 44 kN. Tension absorber (c) is not shown in the plot since it did not trigger in this crash scenario. The successive triggering of the tension absorbers (a) and (b) is caused by the stop option defined in the input-characteristics of the macro elements. At $t = 54$ ms the stop option of the tension absorber (a) is active which forces the triggering of the next tension absorber (b). The constant force level of the tension absorber (a) and (b) in Figure 8b represents smooth energy absorption. In contrast to this, the cabin floor tension absorber (d) shows in Figure 8b a discontinuous force curve that can be compared with Figure 6a to understand the unsteady absorption according to the ovalisation behaviour of the fuselage section. The cabin floor tension absorber triggered at a load level of 25 kN which corresponds approximately to the ultimate load of the passenger crossbeam and therefore the minimum trigger load for controlled failure in case of crash.

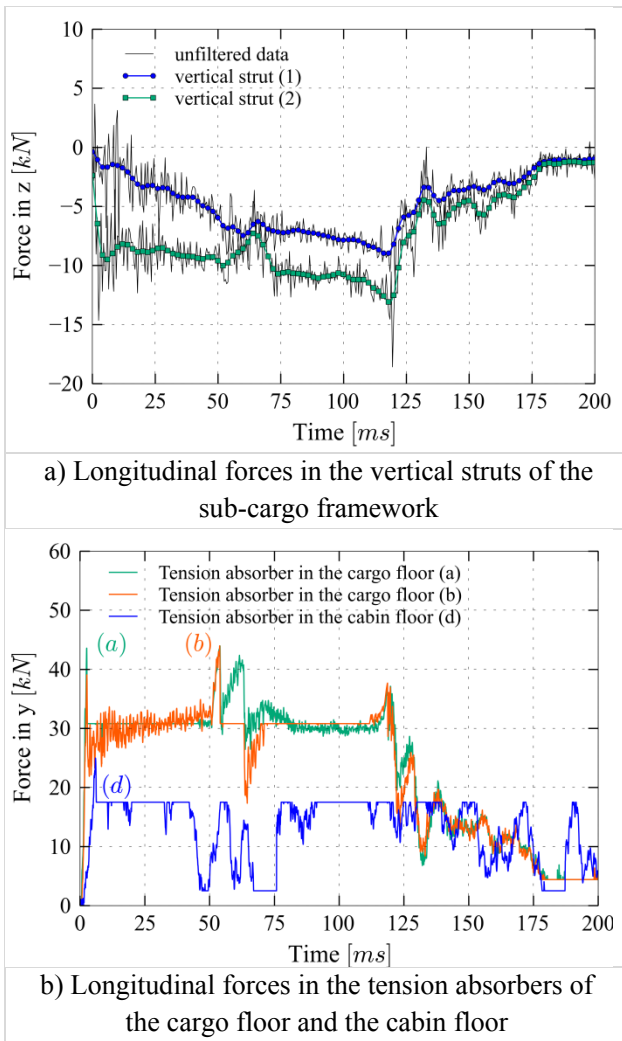


Figure 8: Force and displacement output

Assessment of the passenger loads

In the simulation model the passengers are represented by single mass elements which are connected to the seat structure by spring elements that represent the seat cushion stiffness and the harness system [33], [35]. Non-linear force-displacement characteristics as well as hysteresis behaviour were calibrated on the basis of available test data (e.g. pelvis-cushion compression test) [21]. According to this modelling approach, the acceleration response of the passengers were assessed in an acceleration-time diagram and in an Eiband diagram [8], [10], [16], [17]. The Eiband diagram is obtained by summing the total time of the acceleration level in which an acceleration level is exceeded as it is recommended in [8].

In Figure 9a vertical acceleration responses are illustrated in an acceleration-time diagram. The passengers considered here are located in the first seat row on the left side of the fuselage section and represent an overview on the passenger loads due to the tendency of structural symmetry in the simulation

model. The responses are unfiltered and are sampled with an output frequency of 20 kHz. The passenger at the aisle (PAX 1-C) experiences the largest peak acceleration of 39 g. The passenger next to the window (PAX 1-A) experience a peak acceleration of 38 g. The lowest peak acceleration of 26 g is acting on the passenger in the middle seat (PAX 1-B). With respect to this distribution of passenger loads in a seat row, the cabin floor dynamic behaviour is expected to highly influence the acceleration responses.

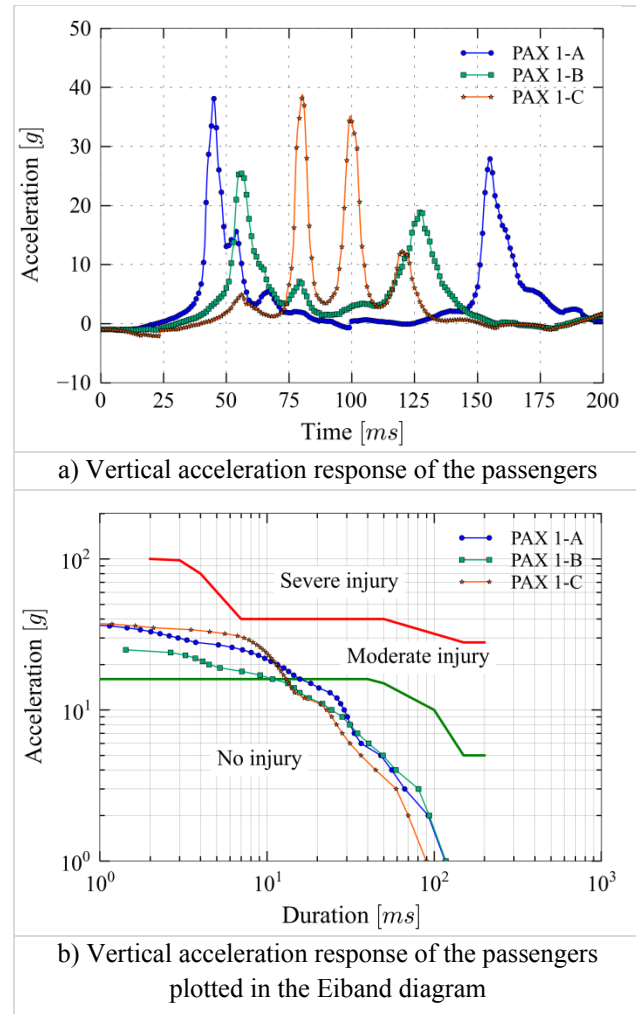


Figure 9: Passenger loads

In Figure 9b the vertical acceleration responses of the considered passengers are plotted in the Eiband diagram. Limit curves of moderate and severe injury for headward acceleration according to Eiband are given in this diagram. The acceleration responses of the passenger at the aisle (PAX 1-C) and next to the window (PAX 1-A) are in the upper region of moderate injury but still distant from the limit of severe injury. The acceleration response of the passenger in the middle seat (PAX 1-B) is next to the limit of moderate injury. Finally, all passenger loads are below the limit of severe injury.

3 Consideration of cargo loading

The development of new crash kinematics requires the consideration of different crash loading conditions to identify the robustness of a crash concept. The tension crash concept was investigated in five different robustness crash cases which are listed in Table 3. The crash kinematics was approved in all considered crash cases. The robustness crash case with cargo loading is the most challenging crash case since the cargo mass influences the efficiency of the tension absorption mechanism in the cargo floor. For that reason, the discussion of robustness loading conditions is focussed here on the cargo loading.

Table 3: Investigated robustness crash cases

Robustness crash case

One-sided loading (of passenger + hatrack masses)

Reduced passenger and hatrack loading (50 %)

Impact roll angle 5°

Higher initial velocity ($v_i = 30$ ft/s)

Cargo loading ($m_{\text{CARGO}} = 946$ kg)

Several drop tests performed in the past were equipped with cargo loading to investigate the interaction between an aircraft fuselage and the cargo loading, and to identify correspondent energy absorption mechanism in the aircraft fuselage [1], [2], [20], [25], [32]. In Figure 10 exemplary drop tests of two aircraft fuselage sections are shown which were loaded in the cargo compartment with bulk luggage respectively with an auxiliary fuel tank. In both cases multiple frame failure and crushing of the sub-cargo structure occurs which results in a flattening crash kinematics of the lower fuselage section. As previously described the kinetic energy is absorbed mainly by plastic deformation of the frame, the sub-cargo structure and the skin.

In this paragraph a crash kinematics is presented in which the influence of the cargo loading on the tension absorption mechanism in the cargo floor is investigated. The cargo loading has large importance in the development of the tension absorption concept since it significantly influences the tension absorption mechanism in the cargo floor. The functionality of the tension crash concept has to be ensured in the case of cargo loading.

In general, diverse cargo types are transported in the cargo hold of the aircraft fuselage. The cargo types distinguish in shape, dimension, stiffness, weight, etc.

To avoid the complexity to consider diverse cargo types with different characteristics, the cargo loading in this preliminary design study is modelled with a simplified approach. In this approach the cargo is modelled as a cuboid of solid reduced integrated elements (width = 1282 mm; length = 1270 mm, height = 375 mm) with linear-elastic material law and a total mass of 946 kg. The cargo model itself absorbs almost no kinetic energy, except of negligible effects of elastically stored energy. Between the cargo floor and the cargo cuboid a contact with a friction coefficient of $\mu = 0.4$ is defined. The influence of an interaction between the cargo and the cabin floor is not considered in this simplified approach. The focus of this simplified modelling approach is on the inertia of the cargo mass and of the correspondent cargo forces acting on the cargo floor structure (with tension absorption mechanism). The functionality of the tension absorption concept in combination with these cargo loads shall be investigated.





| | a) Crash kinematics with bulk luggage in the cargo | b) Crash kinematics with a conformable auxiliary fuel tank |
|----------|--------------------------------------------------------------------------------------|---------------------------------------------------------------------------------------|
| Pretest |  |  |
| Posttest |  |  |
| | <i>FAA crash dynamics and engineering development program [2]</i> | <i>FAA crash dynamics and engineering development program [1]</i> |

Figure 10: Drop tests with cargo loading

The input-characteristics of the macro elements in the cabin floor, in the kinematic hinges and in the cargo floor are the same as described in Figure 3. The lateral cargo struts are extended as shown in Figure 11 and are modelled with an additional tension absorber (e) to achieve sufficient energy absorption and to fulfil the cargo crash case. By the extended lateral struts simultaneous energy absorption in the kinematic

hinges (C) and in the tension absorber (e) is achieved. The input-characteristics of the macro elements in the lateral struts (e) correspond to the input-characteristics of the macro elements in the cargo floor (a), (b), (c).

In case of crash, the cargo mass has to be stopped specifically to prevent the tension absorption mechanism as well as the whole sub-cargo structure from total damage. This is achieved by an installation of vertical orientated, crushable structural elements in the sub-cargo area. The task of the vertical structural elements is to allow limited crushing in case of cargo loading in order to stop the cargo mass on high crush load level within a limited crushing distance. Limited crushing of these vertical struts reduces the maximum load peaks introduced by the cargo mass and prevent the cargo-structure from failure or total collapse. Furthermore, limited crushing of the vertical struts still provides sufficient framework height to obtain tension loads in the cargo floor. The tension absorption mechanism can be installed in the sub-cargo structure such that limited crushing does not affect its functionality.

The input-characteristics of the vertical structural elements is shown in Figure 11. The stiffness S_{uc} , the trigger force in compression direction F_{1c} , the constant absorption force F_{2c} , the trigger force in tension direction F_{3c} and the ratio $\frac{F_{1c}}{F_{2c}} = 0.8$ of the structural elements are assumed values on the basis of idealised experimental tests results obtained from [11], [13], [14], [15], [18], [19], [36]. The vertical structural elements are fixed about the x-axis (flight direction).

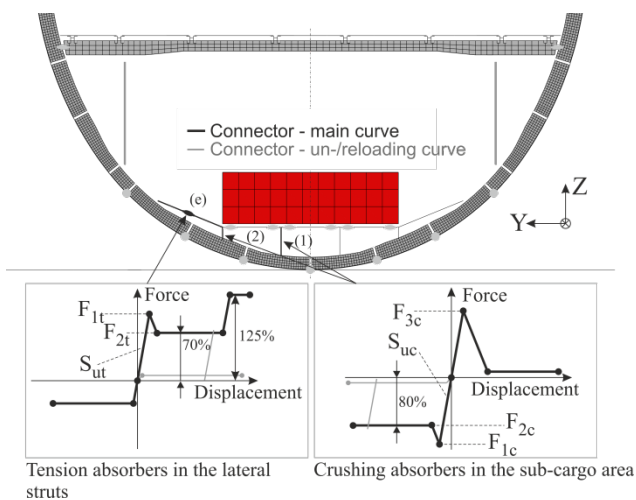


Figure 11: Input-characteristics for the macro elements representing additional structural failure in the cargo floor structure

In Figure 12 the sequence of the crash kinematics is shown. In the first crash phase (up to $t = 50$ ms), the kinematic hinges (A) at the impact point fail which causes the triggering of the tension absorbers (a) in the cargo floor. Increasing crash loads and deformations lead to the triggering of the kinematic hinges (D) and the cabin floor tension absorbers (d) at approximately the same time. The cargo loading initiates progressive crushing of the vertical structural elements (1) and (2) in the sub-cargo area almost simultaneously to the triggering of the tension absorber (a). Increasing crash loads of the cargo mass initiates the triggering of the kinematic hinges (B) and of the tension absorbers (c) (Figure 12b). In the subsequent crash phase kinetic energy is absorbed in the kinematic hinges (A), (B), (D) as well as by tension absorption (a) and (c) in the cargo floor. At the final stage of the crash case additional kinetic energy is absorbed simultaneously in the kinematic hinges (C) and in the tension absorbers (e) which bypasses the kinematic hinges (C).

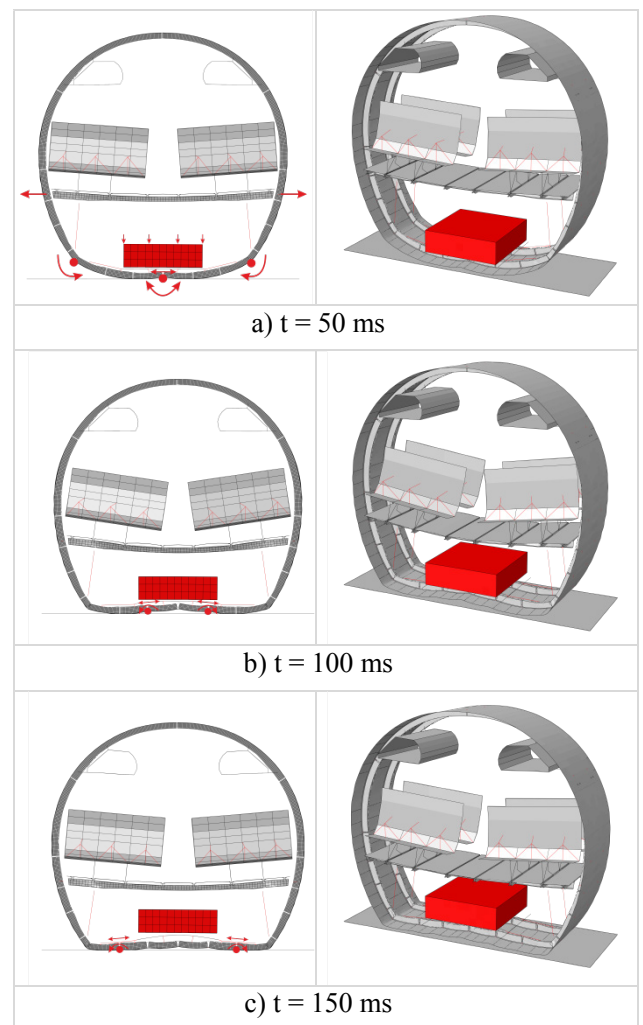


Figure 12: Flattening crash kinematics of the fuselage section loaded with cargo mass

Energy balance

In Figure 13a the energy balance of the simulation model is shown. The total energy E_{TOT} is almost constant at 53.4 kJ which is 1.65 times the initial kinetic energy given in the crash case without cargo loading. At the final crash state ($t_1 = 200$ ms), the initial kinetic energy and the external work $E_{KE}^0 + E_W^1$ (100 %) are transformed to the internal energy E_I^1 (85.1 %) and to the frictional dissipated energy E_{FD}^1 (5.0 %). A remaining kinetic energy E_{KE}^1 (7.4 %) is in the fuselage structure at this final state of the simulation.

At $t = 35$ ms crushing of the vertical structural elements is completed and the kinetic energy of the cargo is approximately zero, which is apparent by changing of the slope of the internal and of the kinetic energy curves. Compared to the crash case without cargo loading the rebound effect of the fuselage section with cargo loading is higher, which is also apparent from the curves of the internal and the kinetic energies at $t = 138$ ms (Figure 13a).

In Figure 13b the absorbed energies of the individual crash devices are illustrated. With respect to the initial kinetic energy and the external work ($E_{KE}^0 + E_W^1$) the amount of the absorbed energy in the cargo floor tension absorbers (a) and (c) is 15.9 % (9.6 kJ). The absolute value is less compared to the crash case without cargo, which is an indication for disturbed tension absorption in the cargo floor due to the cargo loading. This is compensated by absorption of the remaining kinetic energy in the lateral struts (e) 5.8 % (3.5 kJ) and by a higher ovalisation of the fuselage section in the tension absorbers (d) 7.5 % (4.5 kJ). The amount of the absorbed energy in the vertical structural elements (1) and (2) is 23.9 % (14.4 kJ). The amount of the absorbed energy in the kinematic hinges (A) and (B) is 5.7 % (3.5 kJ) and in the kinematic hinges (C) and (D) 12.3 % (7.5 kJ). In total, about 71.1 % (43.0 kJ) of ($E_{KE}^0 + E_W^1$) were absorbed by the macro models of tension absorption, frame failure and progressive crushing. The internal energy (71.1 %) of the macro elements consists of the elastic strain energy (4.8 %) and of the energy dissipated by damage (66.3 %). The amount of elastic strain energy in the linear-elastically modelled fuselage structure, except the macro elements, is 13.8 %. The elastic strain energy of the fuselage section model and the energy dissipated by damage are not shown in the diagram.

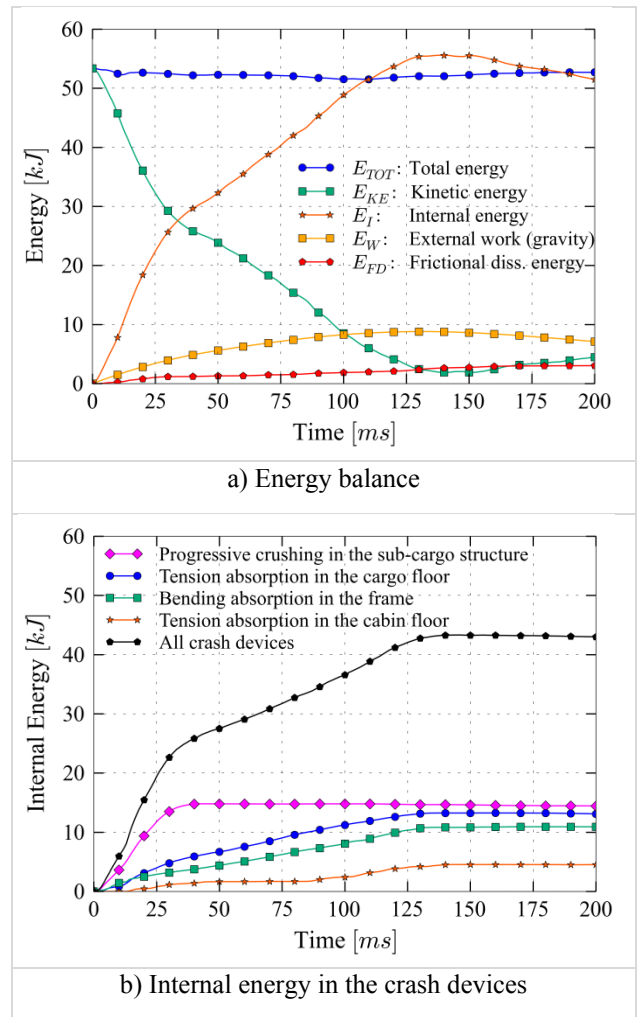


Figure 13: Energy output

Output of the macro elements (displacement in the cargo floor)

The output data of the macro elements can be used to develop or to choose a crush absorber which corresponds to the requirements.

The kinetic energy of the cargo mass is mainly absorbed by progressive crushing of the vertical structural elements while the kinetic energy of the fuselage section is mainly absorbed by tension absorption in the cargo floor and the cabin floor as well as by frame bending.

Figure 14 shows the displacement-time diagram of the crushable macro elements in the sub-cargo area. The maximum longitudinal displacement in the inner and the outer structural elements is reached at $t \approx 35$ ms. The maximum displacement in the inner crush elements (1) is 136 mm and in the outer crush elements 44 mm. The differences in the total crush displacements are given by the fuselage geometry as can be seen in Figure 11. After $t \approx 100$ ms the displacement of the inner crush elements decreases

hence follows the unloading/ reloading curves with negligible force level.

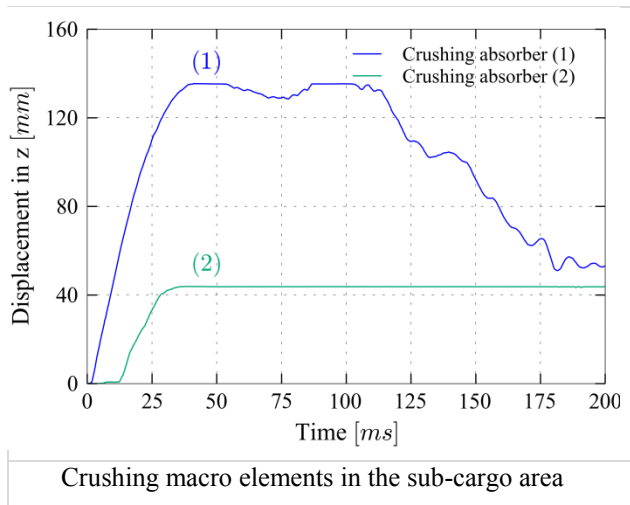


Figure 14: Displacement output data

Assessment of the structural loads in the frame

In the crash case with cargo loading structural adaptations of the frame according to the crash loads was not considered. The frame design corresponds to the one discussed in the crash case without cargo

loading. Instead, the changes of the structural loads compared to the crash case without cargo loading are assessed and the locations of strain exceeding in the frame are identified.

Figure 15 shows the overall and the state plots of the frame longitudinal strains for the crash case with cargo loading. The state plots show the strain in the inner flange of the frame at the most critical states. In the state plots critical exceeding of the strain limits can be identified. At $t = 12.5$ ms and $t = 42$ ms significant strain exceeding occurs in the frame due to the cargo loading which causes high forces in the vertical structural elements, and consequently in the connection between the frame and these crush elements.

Despite of this strain exceeding at the load introduction points of the crushable struts, the overall plot shows strain curves with similar strain limit exceeding compared to the crash case without cargo loading. However, within the strain limits slightly increased strains can be identified in the crash case with cargo loading.

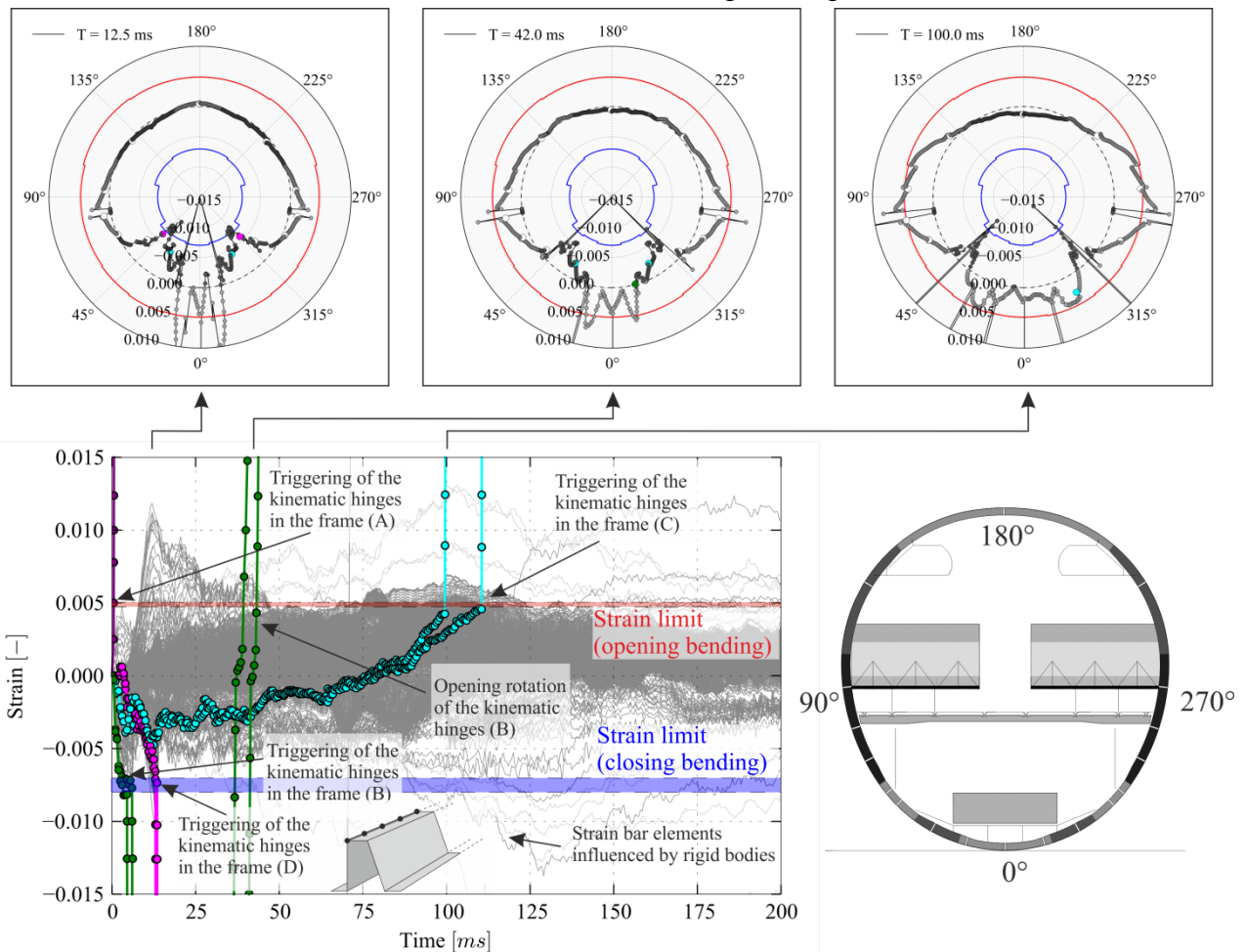


Figure 15: Circumferential strain in the inner flange of the frame (state plots and overall plot)

In the overall plot the triggering of the kinematic hinges is indicated by abrupt increase of the strain in the strain bar elements which are located in the kinematic hinges. The triggering of the kinematic hinges in the robustness crash case with cargo loading is slightly different compared to the crash case without cargo loading. While the kinematic hinges (A), (C) and (D) show similar rotation behaviour, the kinematic hinges (B) trigger already at $t \approx 6$ ms in closing direction with successive closing rotation of 5° (not shown in the diagram). This effect is related to the crushing of the vertical orientated struts in the sub-cargo area. At $t \approx 35$ ms the kinetic energy of the cargo is almost absorbed by the crushable struts and the crash kinematics forces the kinematic hinges (B) to opening rotation similar to the crash kinematics without cargo loading. In Figure 15 the opening rotation of the kinematic hinges (B) is indicated by vertical lines between 35 and 40 ms.

Assessment of the structural loads in the cargo floor

According to the desired crash kinematics, limited crushing of the vertical structural elements in the sub-cargo structure shall occur exclusively in crash cases with cargo loading. Comparably high load levels are required to limit the crushing distance in case of cargo. These crush forces on high level lead to high stresses in the connection of the crushable struts to the frame and hence to the strain exceeding shown in Figure 15. Alternative structural designs could provide a connection of the crushable struts to the fuselage skin to allow load introduction of the crush loads directly to the ground.

Figure 16 shows the force-time diagram of the crushable struts in sub-cargo area. The struts trigger at 25 kN and progressively crush at 80 % of the trigger force. The progressive crushing is completed at $t \approx 40$ ms. At that time most of the initial kinetic energy of the total fuselage section is still kinetic and has to be absorbed in the further crash sequence. Hence, this plot of curves in Figure 16 illustrates that the tension absorption mechanism in the cargo floor has to remain intact after the impact of the cargo mass on the cargo floor.

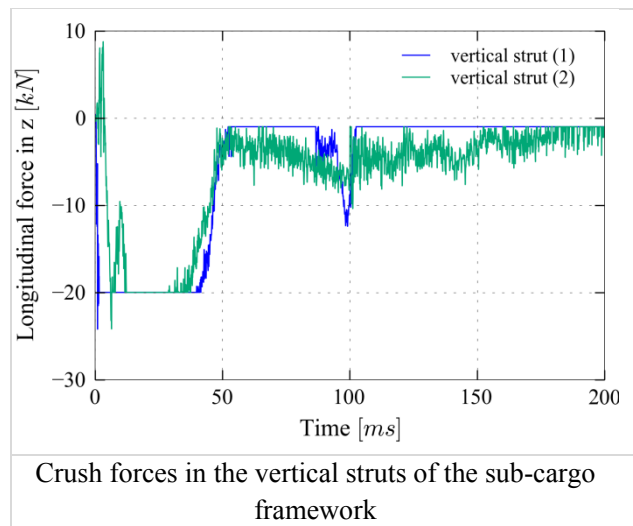
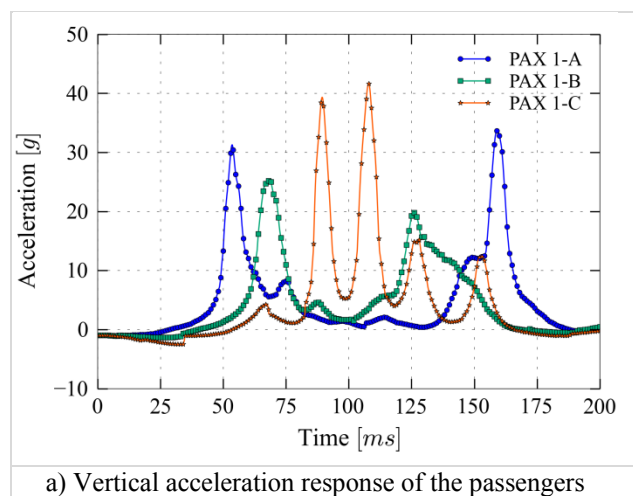


Figure 16: Force output

Assessment of the passenger loads

In Figure 17a the acceleration time diagram of the passengers is illustrated. The maximum acceleration peaks of the passenger in the aisle (PAX 1-C) and of the passenger in the middle seat (PAX 1-B) are slightly increased compared to the crash case without cargo loading. The passenger at the window (PAX 1-A) experiences a smaller maximum peak compared to the crash case without cargo loading. Besides this, the acceleration peaks of all passengers in the crash case with cargo loading are shifted by $\Delta t \approx 10$ ms which means that the passengers in the crash case with cargo loading experiences the maximum acceleration peaks 10 ms later than the passengers in the crash case without cargo loading.

Figure 17b shows the acceleration responses of the passengers in the Eiband diagram. The passenger loads are in moderate injury area and clearly below the limit for severe injury.



a) Vertical acceleration response of the passengers

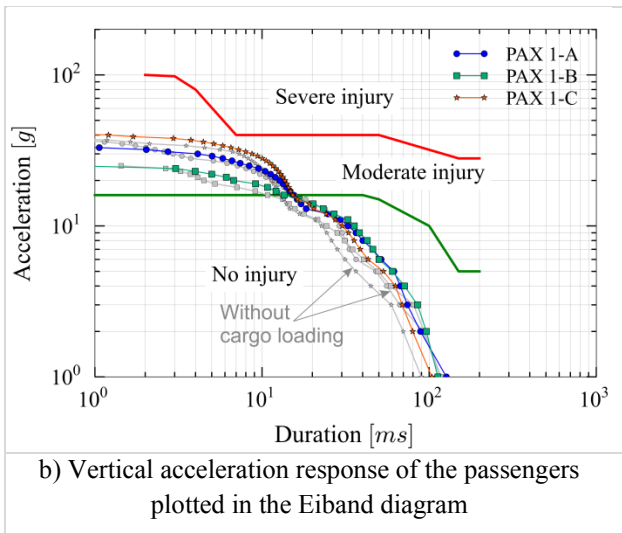


Figure 17: Passenger loads

4 Summary & Conclusion

Crashworthiness research on CFRP transport aircraft performed in the past mainly focused the so called bend-frame concept. In this concept a main part of the kinetic crash energy shall be absorbed by crushing of the sub-cargo structure benefiting from the high mass-specific energy absorption of CFRP failure in the progressive crushing mode. A main drawback of this concept was identified in the massive design of the cargo crossbeam and the frame which is necessary to allow crushing of the sub-cargo structure without failure in the structural regions above. This structural crash design finally leads to significant mass penalty compared to the static sizing that does not consider the crash load case.

An alternative crash concept for CFRP transport aircraft was developed that is discussed in this paper. General research work on crashworthiness of transport aircraft identified high tension forces acting in the cargo crossbeam (due to the global bending of the sub-cargo structure) and in the passenger crossbeam (due to the ovalisation of the fuselage section). The considered alternative crash concept shall benefit from these typical crash loads and absorb a main portion of the kinetic crash energy by tensile absorption mechanisms. With respect to the cargo floor structure, significantly more filigree respectively lightweight designs can be realised with tension absorption compared to the bend-frame concept. In this context, the requirements for energy absorption in the frame were significantly reduced, compared to metallic frame structures, to conform to the brittle failure behaviour of CFRP frames subjected to bending loads. Hence, the alternative crash concept

specifies main energy absorption by tensile loads in the cargo floor and the cabin floor and further limited energy absorption in the frame structure.

The investigation and development of the tension crash concept was conducted on preliminary design level based on a statically sized generic aircraft design. The kinematics model approach was used that allows the description of structural failure by macro models. Using this approach an appropriate crash kinematics was developed with smooth energy absorption and corresponding reduced crash loads. The developed crash kinematics was assessed with respect to structural and passenger loads. In addition, required crash device characteristics were derived from the macro elements output that can be used for the development of local tension absorption mechanisms.

The developed crash concept was further investigated in a robustness crash case with cargo loading. A simplified approach for representation of cargo loading was chosen which is sufficient in this preliminary design phase. With respect to the enormous inertia forces introduced by the cargo mass in the sub-cargo structure, the functionality of the tension absorption mechanism located in the cargo floor has to be ensured. Crushable struts were implemented in the sub-cargo structure to allow limited crushing and accordingly to reduce the crash loads on the cargo floor structure that avoids structural collapse respectively damage of the tension absorbers. Furthermore, a lateral extension of the cargo floor tension absorbers was implemented to improve the energy absorption capacity. The assessment of the improved tension crash concept for cargo loading identified good crash behaviour with comparably smooth energy absorption despite of the cargo mass.

After development and assessment of the crash concept with tension absorption in the cargo and cabin floor the following outcomes can be stated:

- By using comparably simple tension absorption mechanisms a more filigree crashworthy cargo floor structure can be realised compared to the massive backing structure that is necessary for the bend-frame concept.
- The tension crash concept provides acceptable acceleration responses of the passengers as well as moderate structural

loads that lead to comparably small mass penalty due to the crashworthy sizing.

- Parallel activation of the crash devices in the cargo floor, the cabin floor and in the frame results in smooth energy absorption during the whole crash sequence; in contrast to cascading crash concepts that initiate load peaks by triggering of the individual absorptions levels.
- Due to simultaneous energy absorption in all crash devices, different absorption characteristics can be combined flexibly leading to appropriate total energy absorption as required.
- Most of the kinetic crash energy could be absorbed in the tension absorbers of the cargo floor and of the cabin floor.
- Limited requirements for energy absorption in the CFRP frames avoid the integration of complex bending absorber mechanisms in the frame.
- An appropriate crash design could be developed that allows tension absorption in the cargo floor structure despite of cargo loading.
- Potential absorber characteristics could be identified in the simulation study that are necessary to achieve the desired tension crash kinematics. Required load levels for failure initiation, absorption load levels and maximum absorber displacements can be used to develop appropriate absorber concepts.

Acknowledgements

The research leading to these results was accomplished in the framework of the 4th aeronautical research programme of the German Federal Ministry of Economics and Technology (BMWi) under grant 20W1105B, as part of the LuFo-IV project CREVAD (TENOR). The research was conducted in close collaboration with Airbus Operations GmbH and EADS Innovation Works.

The authors wish to thank Dieter Hachenberg and Lars Margull (Airbus) as well as Brian Bautz, Tim Bergmann and Sebastian Heimbs (EADS-IW) for good support provided by technical discussions and information about structural designs.

References

- [1] A. Abramowitz, T. G. Smith, and T. Vu, *Vertical drop test of a narrow-body transport fuselage section with a conformable auxiliary fuel tank onboard*, DOT/FAA/AR-00/56, 2000.
- [2] A. Abramowitz, T. G. Smith, T. Vu, and J. R. Zvanya, *Vertical drop test of a narrow-body transport fuselage section with overhead stowage bins*, DOT/FAA/AR-01/100, 2002.
- [3] G. Beuck, H.-J. Mueller, and R. Schliwa, *Multi-deck passenger aircraft having impact energy absorbing structures*, Patent Application US 5 542 626, 1996.
- [4] R. L. Boitnott, E. L. Fasanella, L. E. Calton, and H. D. Carden, *Impact response of composite fuselage frames*, SAE Technical Paper 871009, 1987.
- [5] R. L. Boitnott and E. L. Fasanella, *Impact evaluation of composite floor sections*, SAE Technical Paper 891018, 1989.
- [6] A. O. Bolukbasi, T. R. Baxter, T. A. Nguyen, M. Rassaian, K. R. Davis, W. Koch, and L. C. Firth, *Energy absorbing structure for aircraft*, Patent application GB 2 444 645 A, 2008.
- [7] D. Delsart, D. Joly, M. Mahe, and G. Winkelmueller, *Evaluation of finite element modelling methodologies for the design of crashworthy composite commercial aircraft fuselage*, in 24th International Congress of the Aeronautical Sciences, Yokohama, Japan, 2004.
- [8] S. P. Desjardins, R. E. Zimmermann, A. O. Bolukbasi, and N. A. Merritt, *Aircraft crash survival design guide - volume IV - aircraft seats, restraints, litters, and cockpit/cabin de-lethalization*, USAAVSCOM TR 89-D-22D, 1989.
- [9] S. P. Desjardins, *The evolution of energy absorption systems for crashworthy helicopter seats*, in American Helicopter Society 59th Annual Forum, Phoenix, Arizona, USA, 2003.
- [10] A. M. Eiband, *Human tolerance to rapidly applied accelerations: a summary of the literature*, NASA MEMO 5-19-59E, 1959.
- [11] G. L. Farley, *Energy absorption of composite materials*, Journal of Composite Materials, vol. 17, no. 3, pp. 267–279, 1983.

- [12] E. L. Fasanella and E. Alfaro-Bou, *Vertical drop test of a transport fuselage section located aft of the wing*, NASA-TM 89025, 1986.
- [13] S. Heimbs, F. Strobl, and P. Middendorf, *Integration of a composite crash absorber in aircraft fuselage vertical struts*, International Journal of Vehicle Structures & Systems, vol. 3, no. 2, pp. 87–95, 2011.
- [14] D. Hull, *A unified approach to progressive crushing of fibre - reinforced composite tubes*, Composites Science and Technology, vol. 40, no. 4, pp. 377–421, 1991.
- [15] A. Jackson, S. Dutton, A. J. Gunnion, and D. Kelly, *Investigation into laminate design of open carbon - fibre/epoxy sections by quasi - static and dynamic crushing*, Composite Structures, vol. 93, no. 10, pp. 2646–2654, 2011.
- [16] K. E. Jackson, E. L. Fasanella, R. L. Boitnott, and K. H. Lyle, *Full-scale crash test and finite element simulation of a composite prototype helicopter*, NASA/TP-2003-212641, 2003.
- [17] K. E. Jackson, E. L. Fasanella, R. L. Boitnott, J. McEntire, and A. Lewis, *Occupant responses in a full-scale crash test of the Sikorsky ACAP helicopter*, Journal of the American Helicopter Society, 2004.
- [18] A. F. Johnson and D. Kohlgrüber, *Design and performance of energy absorbing subfloor structures in aerospace applications*, in IMechE Seminar S672: Materials and Structures for Energy Absorption, London, 2000.
- [19] A. F. Johnson and M. David, *Failure mechanisms in energy-absorbing composite structures*, Philosophical Magazine, vol. 90, no. 31–32, pp. 4245–4261, 2010.
- [20] D. Johnson and A. Wilson, *Vertical drop test of a transport airframe section*, DOT/FAA/CT-TN 86/34, 1986.
- [21] G. L. W. M. Knops, *AERO-CT92-0030/Crashworthiness for commercial aircraft; subtask 2.4: supporting test work aircraft seat component tests*, TNO-report No.: 94.OR.BV.011.1/GKN, 1994.
- [22] I. Kumakura, *Vertical drop test of a transport fuselage section*, SAE Technical Paper 2002-01-2997, 2002.
- [23] I. Kumakura, M. Minegishi, K. Iwasaki, H. Shoji, H. Miyaki, N. Yoshimoto, H. Sashikuma, N. Katayama, A. Isoe, T. Hayashi, T. Yamaoka, and T. Akaso, *Summary of vertical drop tests of YS-11 transport fuselage sections*, 2003.
- [24] F. LePage and R. Carciente, *A320 fuselage section vertical drop test, part 2: test results*, CEAT test report S95 5776/2, European Community funded research project “Crashworthiness for commercial aircraft,” 1995.
- [25] T. V. Logue, R. J. McGuire, J. W. Reinhardt, and T. Vu, *Vertical drop test of a narrow-body fuselage section with overhead stowage bins and auxiliary fuel tank on board*, DOT/FAA/CT-94/116, 1995.
- [26] M. Lützenburger and A. Johnson, *HeliSafe - helicopter occupant safety - development of a composite seat absorber element*, Technical Report D33-2a, 2002.
- [27] M. Lützenburger, *Studies about the utilisation of the aircraft cargo compartment as additional passenger cabin by use of numerical crash simulation*, in The Fifth Triennial International Fire & Cabin Safety Research Conference, Atlantic City, New Jersey, USA, 2007.
- [28] M. Lützenburger, *KRASH related research projects at DLR*, in 6th International KRASH Users’ Seminar, 2009.
- [29] J. Milliere, D. Andissac, C. Raulot, and O. Vincent, *Energy-absorbing structural element made of a composite material and aircraft fuselage having said absorber*, Patent Application US2011/0042513 A1, 2011.
- [30] M. Pein, D. Krause, S. Heimbs, and P. Middendorf, *Innovative energy-absorbing concept for aircraft cabin interior*, in International Workshop on Aircraft System Technologies (AST 2007), Hamburg, Germany, 2007.
- [31] M. Pein, V. Laukart, D. G. Feldmann, and D. Krause, *Concepts for energy absorbing support structures and appropriate materials*, in 25th International Congress of the Aeronautical Sciences, Hamburg, Germany, 2006.
- [32] S. M. Pugliese, *B-707 fuselage drop test report*, Arvin/Calspan Report No. 7252-1 prepared for FAA technical center Atlantic City, 1984.
- [33] M. Waimer, D. Kohlgrüber, D. Hachenberg, and H. Voggenreiter, *The kinematics model – a numerical method for the development of a crashworthy composite fuselage design of transport aircraft*, in The Sixth Triennial

International Aircraft Fire and Cabin Safety
Research Conference, Atlantic City, New Jersey,
USA, 2010.

- [34] M. Waimer, D. Kohlgrüber, R. Keck, and H. Voggenreiter, *Contribution to an improved crash design for a composite transport aircraft fuselage – development of a kinematics model and an experimental component test setup*, CEAS Aeronautical Journal, vol. 4, no. 3, pp. 265–275, 2013.
- [35] M. Waimer, *Development of a kinematics model for the assessment of global crash scenarios of a composite transport aircraft fuselage*, DLR-FB 2013-28, 2013.
- [36] M. Waimer, D. Kohlgrüber, D. Hachenberg, and H. Voggenreiter, *Experimental study of CFRP components subjected to dynamic crash loads*, Composite Structures, vol. 105, pp. 288–299, 2013.
- [37] P. Westphal, W.-D. Dolzinski, T. Roming, T. Schröder, D. Kohlgrüber, and M. Lützenburger, *Strukturbauteil mit Spant- und Querträgerelement*, Patent Application DE 10 2007 030 026 A1, 2009.
- [38] M. S. Williams and R. J. Hayduk, *Vertical drop test of a transport fuselage section located forward of the wing*, NASA TM85679, 1983.
- [39] M. S. Williams and R. J. Hayduk, *Vertical drop test of a transport fuselage center section including the wheel wells*, NASA TM85706, 1983.
- [40] M. B. Woodson, E. R. Johnson, and R. T. Haftka, *Optimal design of composite fuselage frames for crashworthiness*, International Journal of Crashworthiness, vol. 1, no. 4, pp. 369–380, 1996.
- [41] *Federal Aviation Administration: Special conditions: Boeing model B787-8 airplane; Crashworthiness*, US Federal register Vol. 72 No. 111 Docket No. NM368 special conditions No. 25-07-05-SC, 2007.